



ADAM17 mediates ectodomain shedding of the soluble VLDL receptor fragment in the retinal epithelium

Received for publication, May 7, 2021, and in revised form, August 27, 2021 Published, Papers in Press, September 10, 2021, <https://doi.org/10.1016/j.jbc.2021.101185>

Xiang Ma¹, Yusuke Takahashi, Wenjing Wu, Wentao Liang, Jianglei Chen, Dibyendu Chakraborty, Yangxiong Li, Yanhong Du, Siribhinya Benyajati, and Jian-Xing Ma*

From the Department of Physiology, University of Oklahoma Health Sciences Center, Oklahoma City, Oklahoma, USA

Edited by Dennis Voelker

Very low-density lipoprotein receptor (VLDLR) is a multi-functional transmembrane protein. Beyond the function of the full-length VLDLR in lipid transport, the soluble ectodomain of VLDLR (sVLDLR) confers anti-inflammatory and anti-angiogenic roles in ocular tissues through inhibition of canonical Wnt signaling. However, it remains unknown how sVLDLR is shed into the extracellular space. In this study, we present the first evidence that a disintegrin and metalloprotease 17 (ADAM17) is responsible for sVLDLR shedding in human retinal pigment epithelium cells using pharmacological and genetic approaches. Among selected proteinase inhibitors, an ADAM17 inhibitor demonstrated the most potent inhibitory effect on sVLDLR shedding. siRNA-mediated knockdown or CRISPR/Cas9-mediated KO of *ADAM17* diminished, whereas plasmid-mediated overexpression of ADAM17 promoted sVLDLR shedding. The amount of shed sVLDLR correlated with an inhibitory effect on the Wnt signaling pathway. Consistent with these *in vitro* findings, intravitreal injection of an ADAM17 inhibitor reduced sVLDLR levels in the extracellular matrix in the mouse retina. In addition, our results demonstrated that ADAM17 cleaved VLDLR only in cells coexpressing these proteins, suggesting that shedding occurs in a *cis* manner. Moreover, our study demonstrated that aberrant activation of Wnt signaling was associated with decreased sVLDLR levels, along with down-regulation of ADAM17 in ocular tissues of an age-related macular degeneration model. Taken together, our observations reveal the mechanism underlying VLDLR cleavage and identify a potential therapeutic target for the treatment of disorders associated with dysregulation of Wnt signaling.

Very low-density lipoprotein receptor (VLDLR) is a multi-functional protein in the low-density lipoprotein receptor (LDLR) family (1). It is originally recognized to mediate VLDL binding and lipid uptake in extrahepatic tissues, where it plays a vital role in lipoprotein metabolism (2, 3). VLDLR also serves as the receptor for reelin and clusterin, which are involved in brain pathophysiology (4, 5). Recently, our group identified the VLDLR ectodomain as an endogenous inhibitor of canonical Wnt signaling through binding with the Wnt coreceptor,

low-density lipoprotein receptor-related protein 6 (LRP6) (6, 7). In addition, *Vldlr* gene KO results in Wnt signaling overactivation and subsequently pathological angiogenesis and inflammation (6, 8). These diverse functions of VLDLR can be explained by its multiple isoforms generated *via* alternative splicing and its ectodomain shedding occurring during post-translational modification.

VLDLR is subjected to alternative splicing (9). VLDLR variant I (VLDLRI) is encoded by the full-length VLDLR gene and mediates more efficient VLDL uptake than VLDLR variant II (VLDLRII) (9). VLDLRII lacks the O-linked sugar domain encoded by exon 16 and confers a higher ectodomain shedding rate than VLDLRI and thus demonstrates a more potent Wnt inhibitory effect (10). While most tissues, such as the brain, kidney, and skeletal muscle, express both VLDLRI and VLDLRII, the retina expresses exclusively VLDLRII (10), suggesting a unique function of shed ectodomain of VLDLRII in the retina. Thus, we mainly focused on investigating VLDLRII in this study. Previously, we showed that soluble N-terminal ectodomain of VLDLR (sVLDLR) is naturally present in the interphotoreceptor matrix (IPM), the extracellular matrix between the photoreceptors and retinal pigment epithelium (RPE) (10). However, it remains unclear how sVLDLR is released and which proteinase is responsible for VLDLR shedding.

Proteinases that cleave and release the ectodomain of transmembrane proteins into the extracellular space are referred to as sheddases (11). A disintegrin and metalloproteinases (ADAMs) and matrix metalloproteinases (MMPs) are two prominent families of sheddases responsible for the shedding of single-span transmembrane proteins, such as LDLR (12). In addition to abolishing the original functions of transmembrane proteins, the shed ectodomain assumes distinct biological functions in an autocrine or a paracrine manner, such as transforming growth factor alpha and tumor necrosis factor alpha (TNF α) (11). These released extracellular peptides confer regulatory roles in various aspects, such as tissue homeostasis, cell adhesion, signaling transduction, and membrane protein turnover (11). Therefore, sheddases, the crucial players of post-translational modification on transmembrane proteins, must be tightly regulated in physiological conditions. Dysregulated sheddases contribute to the pathological changes in human diseases (11).

* For correspondence: Jian-Xing Ma, jian-xing-ma@ouhsc.edu.

ADAM17 responsible for VLDLR shedding

Age-related macular degeneration (AMD) is the leading cause of irreversible blindness worldwide (13, 14). Although genetic and environmental factors have been associated with the development of AMD, the etiology and pathogenesis of AMD remain largely unknown. Recently, dysfunctional MMPs have been reported to be associated with AMD in human beings (15–17). Genome-wide association studies showed that variations on tissue inhibitor of metalloproteinase 3 (TIMP3) are associated with the onset of AMD (15). Dysregulated expression of ADAMs was reported in the RPE–choroid complex of patients with AMD (16). In addition, the latest study showed that loss of ADAM17, one of intensively studied ADAM members, promotes AMD-like phenotypes (17). These studies indicated that dysregulation of sheddases might be implicated in the etiology of AMD. Combined with our recent work showing that overactivated Wnt signaling was detected in the macula of patients with AMD (18), we proposed that downregulation of the VLDLR sheddase contributes to the reduced sVLDLR level and overactivated canonical Wnt signaling, which may play a role in the AMD pathogenesis.

In this study, we aimed to identify the sheddase responsible for sVLDLR release using pharmacological and genetic approaches. We first screened for the potential sheddases using various proteinase inhibitors. We then identified VLDLR sheddase by loss-of-function approaches using siRNA-mediated knockdown and CRISPR/Cas9 KO technology and by a gain-of-function approach using plasmid overexpression. We also validated the sheddase identification *in vivo*. Moreover, we tested if regulation of the VLDLR sheddase can control the sVLDLR-mediated inhibitory effect on Wnt signaling. Finally, we revealed the association of the VLDLR sheddase-mediated VLDLR shedding with the activation of Wnt signaling under AMD conditions.

Results

Effects of a proteinase activator and various inhibitors on VLDLR shedding

To screen for the candidate proteinase responsible for VLDLR shedding, we applied one sheddase activator and four sheddase inhibitors covering the majority of sheddase families, MMPs and ADAMs. Phorbol 12-myristate 13-acetate (PMA), a protein kinase C (PKC) activator, was reported to induce the shedding of certain membrane-anchored proteins, including meprins (10, 19). In this study, we found that PMA increased VLDLRII shedding, indicating that PKC activation promoted the activity of the VLDLR sheddase (Fig. 1A). TNF α proteinase inhibitor 1, a broad-spectrum inhibitor of MMPs and ADAMs, markedly reduced VLDLRII shedding (Fig. 1A). In addition, VLDLRII shedding was unaffected by GM6001, a pan-MMP inhibitor, indicating that MMPs were not involved in VLDLR shedding, and ADAMs may be responsible for VLDLR shedding (Fig. 1A). Among the ADAM family, ADAM10 and ADAM17 are well known for regulating the shedding of integral membrane proteins (11). Also, PKC is a potent inducer for both ADAM10 and ADAM17 (19, 20). To identify the

member of the ADAM family that cleaves VLDLR, two ADAM inhibitors with different IC₅₀ for ADAM10 and ADAM17 were used, including GI254023x (IC₅₀ = 5.3 nM for ADAM10 and IC₅₀ = 541.0 nM for ADAM17) and GW280264x (IC₅₀ = 11.5 nM for ADAM10 and IC₅₀ = 8.0 nM for ADAM17) (21). Both GI254023x and GW280264x demonstrated significant inhibitory effects on VLDLRII shedding (Fig. 1, A and B). With the same concentration of these inhibitors, GW280264x demonstrated the most potent inhibitory effect on VLDLRII shedding compared with other proteinase inhibitors. We also demonstrated that GW280264x dose dependently inhibited VLDLRII shedding (Fig. 1, C and D) and ADAM17 activity (Fig. 1E) in primary human RPE cells. Moreover, we found that GW280264x suppressed VLDLR shedding in other cell types, including retinal cells (R28 cell line with a photoreceptor origin), renal cells (human embryonic kidney 293 cell line), and endothelial cells (human umbilical vein endothelial cells) (Fig. S1, A and B). In addition to VLDLRII, we found that VLDLRI shedding was suppressed most effectively with GW280264x relative to other sheddase inhibitors (Fig. S2, A and B). These results suggested that ADAM17 were possible sheddases responsible for VLDLR shedding in various cell types.

VLDLR shedding was affected by ADAM17 expression

We next investigated the effect of ADAM10 and ADAM17 on VLDLR shedding using siRNA knockdown of these two ADAMs. As shown in Figure 2A, the ADAM10 siRNA downregulated ADAM10 protein levels by approximately 80%, and the ADAM17 siRNA induced a more than 70% reduction of ADAM17 protein levels in human RPE cells. The ADAM10 siRNA showed no effect on VLDLR shedding, whereas there was a marked reduction of VLDLR shedding in the ADAM17 siRNA-treated cells, indicating that ADAM17 was responsible for VLDLR shedding (Fig. 2, A and B).

To further confirm this finding, we applied plasmids to overexpress ADAM10 and ADAM17. Plasmid ADAM10 and ADAM17 increased protein levels of ADAM10 and ADAM17, respectively (Fig. 2C). While overexpression of ADAM10 did not affect VLDLR shedding, overexpression of ADAM17 promoted VLDLR shedding, confirming that ADAM17, instead of ADAM10, was the VLDLR sheddase (Fig. 2C). In addition, increased VLDLR shedding induced by plasmid-mediated overexpression of ADAM17 was impeded by the ADAM17 siRNA knockdown (Fig. 2E). Levels of sVLDLR in culture media correlated with protein levels of ADAM17 in cell lysates (Fig. 2, E and F).

CRISPR/Cas9-mediated ADAM17 KO blocked VLDLR shedding and its inhibitory effect on Wnt signaling

A human RPE cell line (ARPE-19) with CRISPR/Cas9-mediated *ADAM17* KO was generated (Fig. S3A) to verify that ADAM17 was the sheddase responsible for VLDLR shedding. As shown in Figure 3A, sVLDLR released into culture media of the *ADAM17* KO cells was markedly decreased and barely detected in the *ADAM17* KO cells. Moreover, in

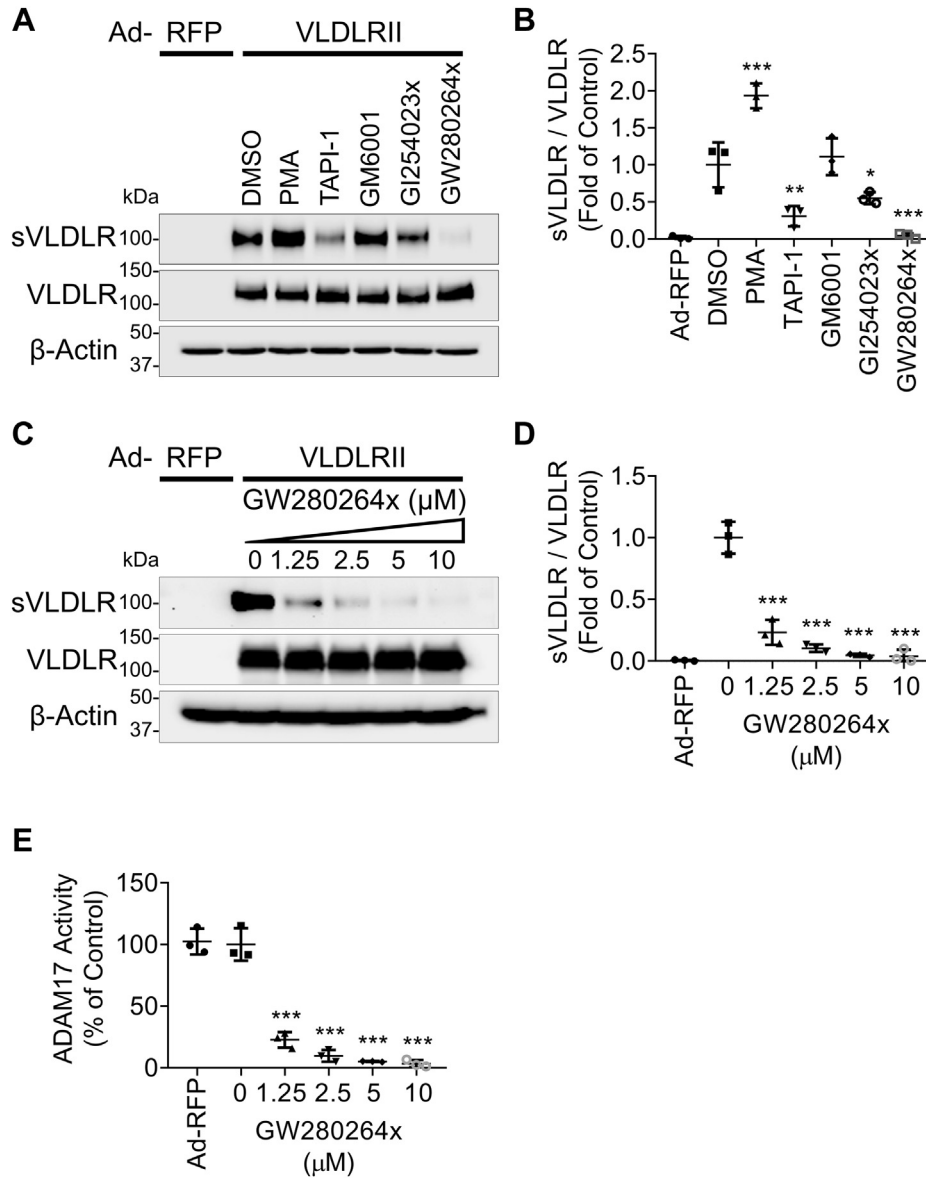


Figure 1. Effect of various proteinase inhibitors on VLDLR shedding. Primary human RPE cells were transduced with adenovirus (MOI = 25) expressing VLDLR^{II} (Ad-VLDLR^{II}) or with Ad-RFP as control for 24 h. Then, culture media were replaced by serum-free DMEM containing various proteinase inhibitors (10 μM) for another 24 h. After that, the culture media and cell lysates were harvested for Western blot analysis. *A*, representative images of Western blotting for soluble ectodomain of VLDLR (sVLDLR) in culture media and the full-length VLDLR in cell lysates. PMA (a PKC activator) and proteinase inhibitors including TAPI-1 (tumor necrosis factor-α proteinase inhibitor), GM6001 (pan-MMP inhibitor), GI254023x (ADAM10 inhibitor), and GW280264x (ADAM17 inhibitor) were used. The same volume of DMSO (vehicle) was used as control. *B*, densitometry analysis of sVLDLR in culture media normalized by the full-length VLDLR levels in cell lysates in (*A*) (n = 3). Cells with Ad-VLDLR^{II} transduction and DMSO treatment were used as control. *C*, representative images of Western blotting for sVLDLR and VLDLR from primary human RPE cells treated with indicated doses of GW280264x or DMSO as control for 24 h. *D*, densitometry of sVLDLR and VLDLR from primary human RPE cells treated with indicated doses of GW280264x or DMSO as control for 24 h. *E*, ADAM17 activity in GW280264x-treated cells were measured using an ADAM17 activity assay kit (n = 3). Data were presented as mean ± SD. **p* < 0.05, ***p* < 0.01, and ****p* < 0.001. ADAM17, a disintegrin and metalloprotease 17; DMEM, Dulbecco's modified Eagle's medium; DMSO, dimethyl sulfoxide; MOI, multiplicity of infection; PKC, protein kinase C; PMA, phorbol 12-myristate 13-acetate; RFP, red fluorescent protein; RPE, retinal pigment epithelium; VLDLR, very low-density lipoprotein receptor; VLDLR^{II}, VLDLR variant II.

these ADAM17 KO cells, plasmid-mediated ADAM17 overexpression restored ADAM17 levels in cell lysates and shed sVLDLR into culture media (Fig. 3, C and D). Taken together, these results further verified that ADAM17 was the sheddase responsible for VLDLR shedding.

Our previous study showed that VLDLR shed its ectodomain, sVLDLR, to confer an inhibitory effect on canonical Wnt signaling through binding with a Wnt coreceptor, LRP6 (7). In this study, we also applied luciferase-based β-catenin

transcriptional activity assay to investigate the effect of ADAM17-regulated sVLDLR release on Wnt pathway activation. Wnt3a-induced T-cell factor (TCF)/β-catenin activity was inhibited by Ad-VLDLR-mediated VLDLR overexpression (Fig. 4A). Overexpression of ADAM17 enhanced the inhibitory effect of VLDLR on Wnt signaling, indicating that ADAM17-induced accumulation of sVLDLR in culture media conferred the inhibitory effect on Wnt signaling (Fig. 4A). Ad-VLDLR induced potent Wnt signaling inhibitory effect in WT

ADAM17 responsible for VLDLR shedding

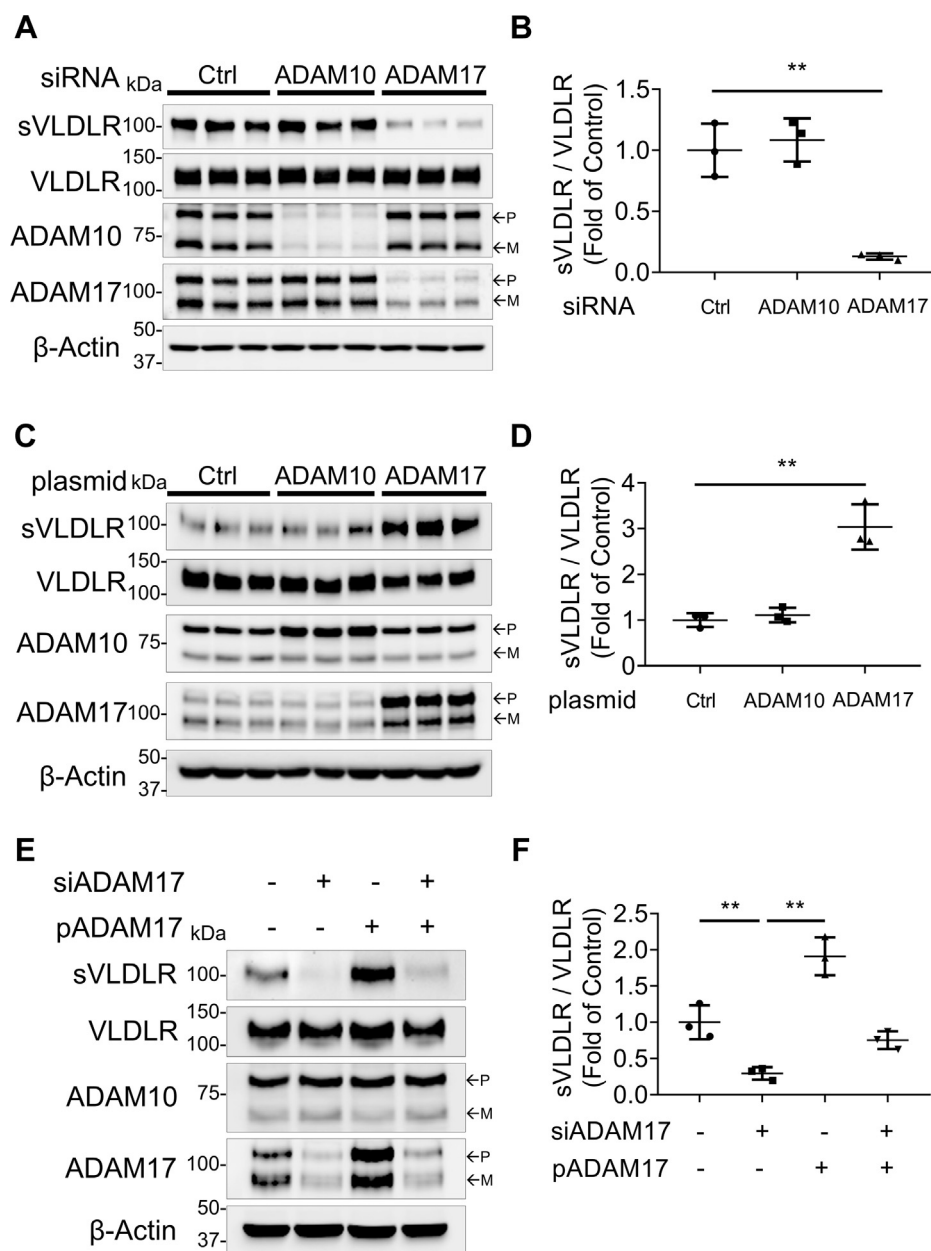


Figure 2. Effect of siRNA knockdown and plasmid overexpression of ADAM10 and ADAM17 on VLDLR shedding. Primary human RPE cells were transiently transfected with indicated siRNA (50 nM) or plasmid (1 μ g/ml) for 24 h. Cells were subsequently infected with Ad-VLDLR_{II} (MOI = 25) for 24 h. Then, culture media were replaced with serum-free DMEM for another 24 h. Finally, culture media and cell lysates were collected for Western blot analysis. *A*, representative images of Western blotting for sVLDLR in culture media and full-length VLDLR, ADAM10, and ADAM17 in cell lysates. The RPE cells were transfected with the siRNA for ADAM10, ADAM17, or control siRNA. *B*, quantification of densitometry of sVLDLR in culture media normalized by VLDLR in cell lysates in (*A*) ($n = 3$). *C*, representative images of Western blotting for sVLDLR in culture media, and VLDLR, ADAM10, and ADAM17 in cells transfected with plasmid overexpressing human ADAM10, human ADAM17, or RFP as control. *D*, protein levels of sVLDLR in the media in (*C*) were quantified and normalized by the full-length VLDLR in cell lysates ($n = 3$). *E*, representative images of Western blotting of sVLDLR in culture media, VLDLR, ADAM10, and ADAM17 in human primary RPE cells, which were transfected with siRNA knocking down human ADAM17 (siADAM17) or plasmid overexpressing human ADAM17 (pADAM17). *F*, quantification of densitometry of sVLDLR in culture media normalized by VLDLR in cell lysates in (*E*) ($n = 3$). In *A*, *C*, and *E*, p and m indicated precursor and mature forms of ADAM10 and ADAM17, respectively. Data were presented as mean \pm SD. ****** $p < 0.01$. ADAM10, a disintegrin and metalloprotease 10; ADAM17, a disintegrin and metalloprotease 17; DMEM, Dulbecco's modified Eagle's medium; MOI, multiplicity of infection; RFP, red fluorescent protein; RPE, retinal pigment epithelium; sVLDLR, soluble ectodomain of VLDLR; VLDLR, very low-density lipoprotein receptor; VLDLR_{II}, VLDLR variant II.

ARPE-19 cells, whereas the Wnt signaling inhibitory effect of Ad-VLDLR was abolished by ADAM17 KO (Fig. 4B). These results strongly supported our hypothesis that sheddase-mediated VLDLR shedding played an important role in modulation of Wnt signaling.

ADAM17 KO enhanced VLDLR-mediated lipid accumulation and reactive oxygen species generation

As the full-length VLDLR plays a crucial role in lipid uptake and deposition in extrahepatic tissues (1), we next investigated if ADAM17-mediated VLDLR shedding has an impact on lipid

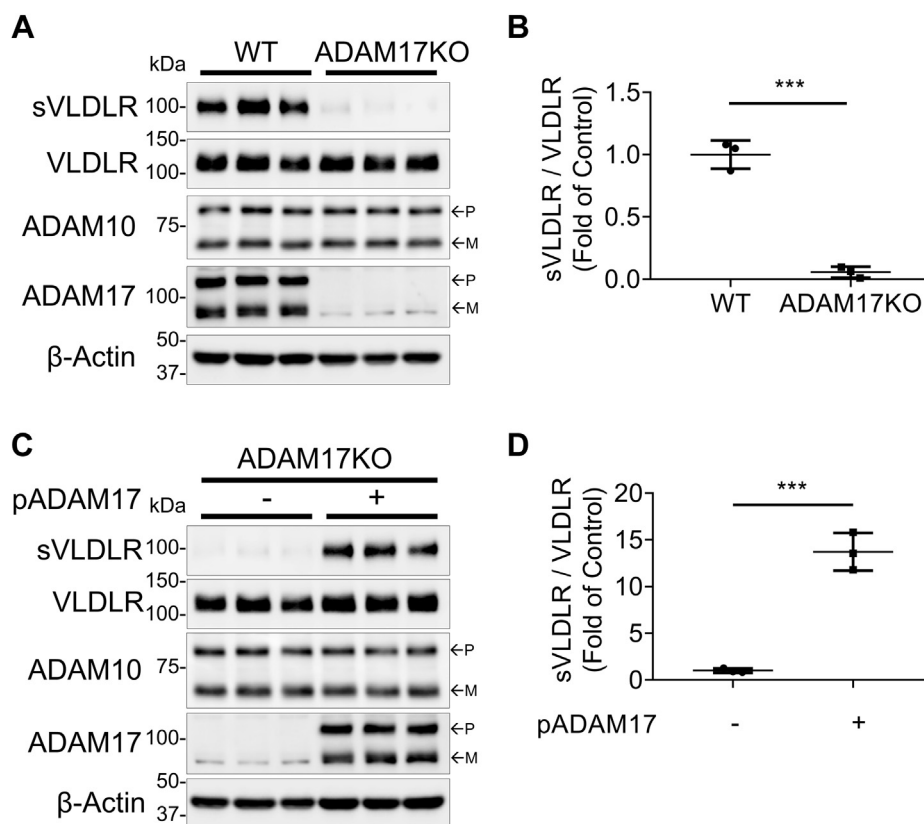


Figure 3. CRISPR/Cas9-mediated ADAM17 KO blocked VLDLR shedding and its effect on Wnt signaling. A, representative images of Western blotting of sVLDLR in the media, and VLDLR, ADAM10, and ADAM17 in cell lysates of Ad-VLDLRII-infected WT and ADAM17 KO ARPE-19 cells. WT cells and ADAM17 KO cells were transfected with Ad-VLDLRII (MOI = 25) for 24 h. Then, culture media were replaced with serum-free DMEM for another 24 h. After that, the conditioned media and cell lysates were harvested for Western blot analysis. B, quantification of densitometry of sVLDLR in culture media normalized by VLDLR in cell lysates in (A) (n = 3). C, representative images of Western blotting of sVLDLR in culture media, and VLDLR, ADAM10, and ADAM17 in cell lysates in ADAM17 KO cells that were transfected with plasmid overexpressing ADAM17 (pADAM17) or RFP as control. D, quantification of densitometry of sVLDLR in culture media normalized by VLDLR in cell lysates in (C) (n = 3). In A and C, p and m indicated precursor and mature forms of ADAM10 and ADAM17, respectively. Data were presented as mean ± SD. ***p < 0.001. ADAM10, a disintegrin and metalloprotease 10; ADAM17, a disintegrin and metalloprotease 17; DMEM, Dulbecco's modified Eagle's medium; MOI, multiplicity of infection; RFP, red fluorescent protein; sVLDLR, soluble ectodomain of VLDLR; VLDLR, very low-density lipoprotein receptor.

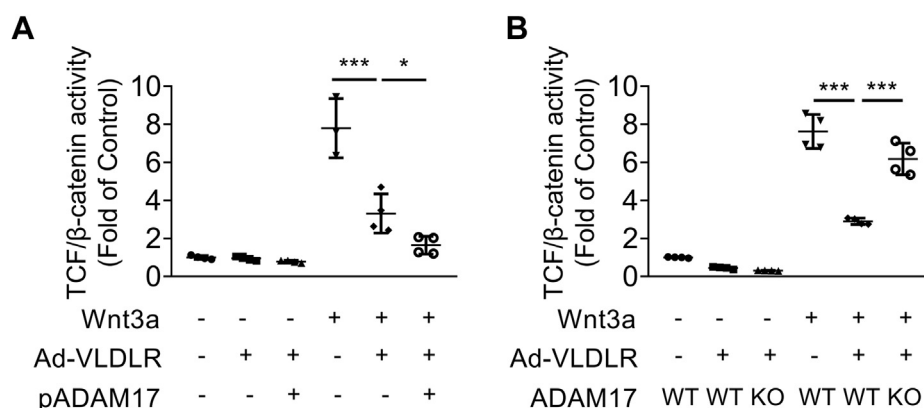


Figure 4. ADAM17 KO blocked the inhibitory effect of VLDLR on Wnt signaling. A, TCF/β-catenin activity was measured in WT ARPE-19 cells with different treatments. Cells were transfected with TOPFLASH reporter plasmid and ADAM17 expression plasmid for 24 h. Then, cells were transfected with Ad-VLDLRII (MOI = 25) or Ad-RFP for 24 h. After that, cells were treated with 20% Wnt3a conditioned media or control conditioned media for 16 h and then collected for TOPFLASH assay (n = 3–4). B, TCF/β-catenin activity was measured in WT ARPE-19 cells and ARPE-19 cells with ADAM17 KO. Cells were transfected with TOPFLASH reporter plasmid for 24 h. Then, cells were transfected with Ad-VLDLRII (MOI = 25) or Ad-RFP for 24 h. After that, cells were treated with 20% Wnt3a conditioned media or control conditioned media for 16 h and then harvested for TOPFLASH assay (n = 4). Data were presented as mean ± SD. *p < 0.05, ***p < 0.001. ADAM17, a disintegrin and metalloprotease 17; MOI, multiplicity of infection; RFP, red fluorescent protein; TCF, T-cell factor; VLDLR, very low-density lipoprotein receptor; VLDLRII, VLDLR variant II.

ADAM17 responsible for VLDLR shedding

uptake. The oleic acid was used to induce intracellular lipid droplet accumulation in this study. BODIPY was used to stain the lipid droplet accumulated in the cytosol. As shown by BODIPY staining, oleic acid dose dependently increased lipid droplets in WT ARPE-19 cells from dose range of 100 to 400 μ M (Fig. S4, A and B). Oleic acid also upregulated reactive oxygen species (ROS) production in a dose-dependent manner (Fig. S4, C and D). Thus, the dose of 200 μ M oleic acid was selected for the following study. Lipid accumulation and ROS generation were measured in oleic acid-treated WT and *ADAM17* KO ARPE-19 cells. As shown in Figure 5, A and B, *ADAM17* KO increased BODIPY-positive area in the cytosol relative to WT ARPE-19 cells. VLDLR overexpression

enhanced the lipid droplet accumulation, which was promoted by *ADAM17* ablation. Similarly, under the treatment of oleic acid, *ADAM17* KO alone increased ROS production compared with WT cells (Fig. 5, C and D). *ADAM17* KO enhanced VLDLR-mediated ROS generation (Fig. 5, C and D). Taken together, these results indicated that VLDLR-mediated lipid uptake and ROS generation were increased by *ADAM17* KO.

ADAM17 functioned as the VLDLR sheddase in vivo

We next examined the effect of GW280264x, an *ADAM17* inhibitor, on VLDLR shedding in ocular tissues of WT C57BL/6J mice. The IPM, the extracellular space between retinal

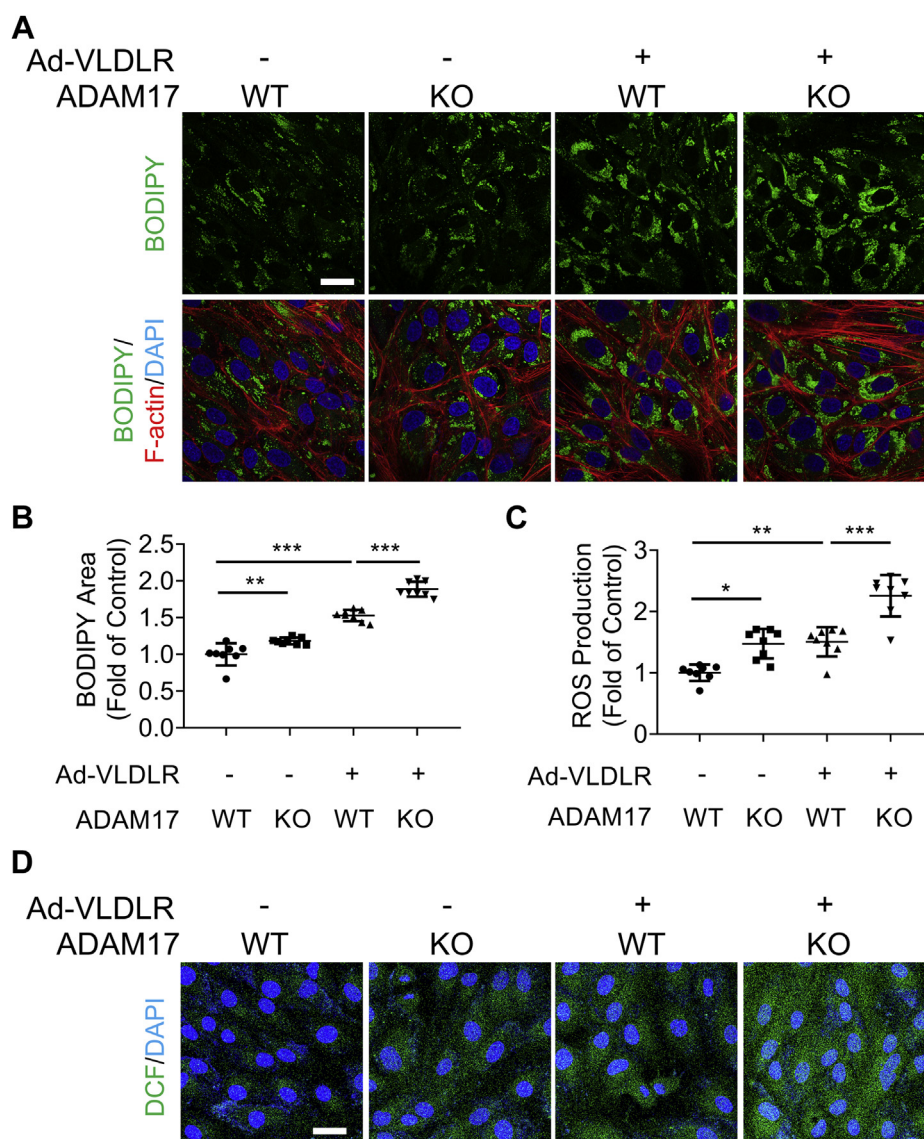


Figure 5. *ADAM17* KO enhanced VLDLR-mediated lipid accumulation and ROS generation. A, representative images of BODIPY-stained lipid droplets (green), phalloidin-stained F-actin (red), and DAPI-stained nuclei in ARPE-19 cells with indicated treatment. Briefly, WT ARPE-19 cells or ARPE-19 cells with *ADAM17* KO were transduced with Ad-VLDLR II (MOI = 25) or Ad-RFP as control for 24 h. Then, cells were treated with BSA-conjugated oleic acid (200 μ M) for 24 h. The scale bar represents 20 μ m. B, areas of lipid droplet areas were quantified according to the BODIPY-positive pixels. BODIPY-positive pixels were normalized by cell number in each image. Data were presented as the fold of control (vehicle group) (n = 8). C, ROS production was measured in ARPE-19 cells with indicated treatment (n = 8). D, representative images of ROS staining in ARPE-19 cells. WT ARPE-19 cells or *ADAM17* KO ARPE-19 cells were transduced with Ad-VLDLR II (MOI = 25) or Ad-RFP as control for 24 h. Then, cells were treated with BSA-conjugated oleic acid (200 μ M) for 24 h. The scale bar represents 20 μ m. Data were presented as mean \pm SD. **p* < 0.05, ***p* < 0.01, and ****p* < 0.001. *ADAM17*, a disintegrin and metalloprotease 17; BSA, bovine serum albumin; DAPI, 4',6'-diamino-2-phenylindole; MOI, multiplicity of infection; RFP, red fluorescent protein; ROS, reactive oxygen species; VLDLR, very low-density lipoprotein receptor.

photoreceptor cells and RPE, plays a crucial role in maintaining the homeostasis of the retina and RPE layer (22). Thus, we intended to determine if the intravitreal injection of GW280264x affects sVLDLR levels in the IPM. Three days after intravitreal injection of GW280264x, the IPM and eyecup (retina–RPE–choroid complex) were collected. Levels of sVLDLR in the IPM were evaluated after normalization to total protein levels in the IPM measured by Ponceau S staining. As shown in Figure 6, GW280264x significantly decreased sVLDLR levels in the IPM compared with the vehicle group. This result provided the *in vivo* evidence supporting that ADAM17 was responsible for VLDLR shedding.

ADAM17 cleaved VLDLR in a cis manner, which was impeded by O-glycosylation of VLDLR

It was critical to understand the cleavage manner of ADAM17 in RPE cells, as RPE–RPE interactions were delicately regulated to maintain their physiological functions in the eyes (23). For the *cis* manner, cells overexpressing both VLDLR and ADAM17 were mixed with the same number of cells overexpressing red fluorescent protein (RFP). For the *trans* manner, cells overexpressing VLDLR were mixed with the same number of cells overexpressing ADAM17. As shown

in Figure 7A, there was an increase of VLDLR shedding in ADAM17 *cis* group compared with control group. ADAM17 *trans* overexpression did not result in increased VLDLR shedding (Fig. 7, A and B). Moreover, we found that the restoration of ADAM17 in a *cis* manner, instead of in a *trans* manner, increased the VLDLR shedding in ADAM17 KO ARPE-19 cells (Fig. S5, A and B). These results indicated that ADAM17 cleaved VLDLR only in a *cis* manner.

We next examined if ADAM17 function was affected by VLDLR O-glycosylation. A mutant Chinese hamster ovary cell line (IdID) with the defect in O-glycosylation was used. As shown in Figure 7, C and D, the ADAM17 overexpression-mediated sVLDLR shedding was blocked by restoration of O-glycosylation using D-(+)-galactose and N-acetyl-D-galactosamine, indicating that glycosylation has a negative effect on ADAM17-mediated VLDLR shedding.

AMD stressor reduced VLDLR shedding by downregulating ADAM17 levels

It was reported that ADAM17 levels were reduced in the RPE of dry AMD patients compared with those of healthy controls (16). A₂E, bisretinoid N-retinyl-N-retinylidene ethanolamine, is an abnormal fluorescent condensation byproduct

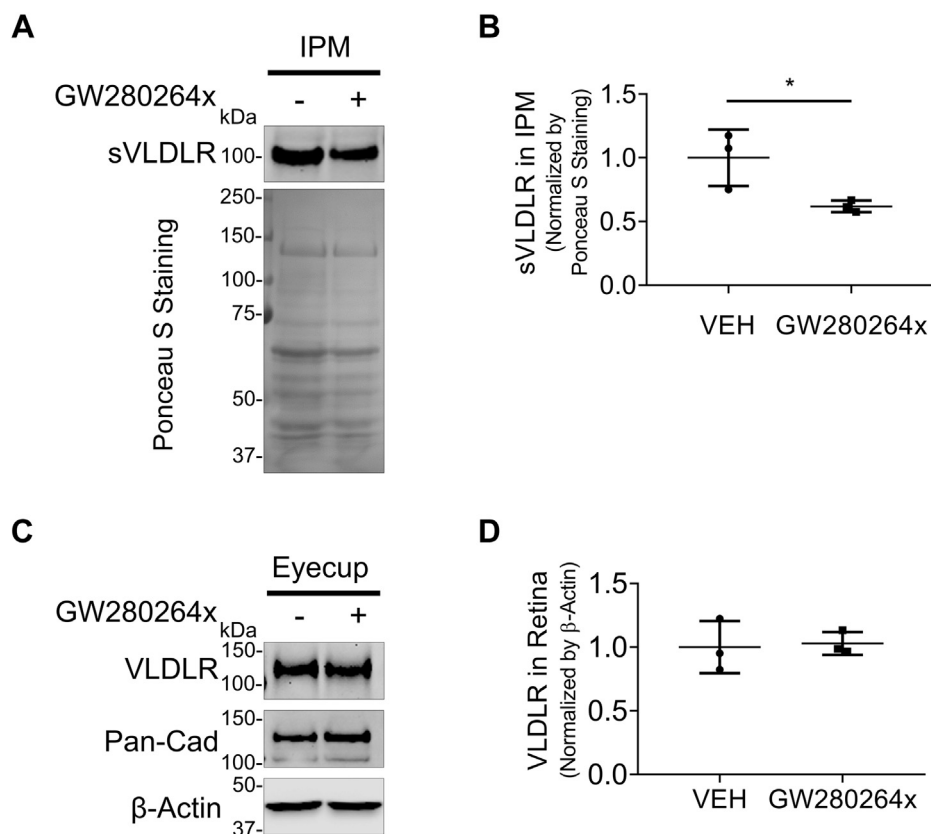


Figure 6. Establishment of ADAM17 as VLDLR sheddase *in vivo*. Two-month-old WT C57BL/6J mice were intravitreally injected with 1.5 μ l GW280264x (2 mM) or the same volume of DMSO (vehicle) as control. Three days later, the interphotoreceptor matrix (IPM) and retinas were harvested for Western blot analysis. A, representative images of Western blotting of sVLDLR in the IPM and Ponceau S staining of its nitrocellulose membrane. B, densitometry quantification of sVLDLR in the IPM normalized by total proteins measured by Ponceau S staining in (A) ($n = 3$). C, representative images of Western blotting of full-length VLDLR and pan-cadherin in the eyecup. D, densitometry quantification of VLDLR normalized by β -actin in the eyecup in (C) ($n = 3$). Data were presented as mean \pm SD. * $p < 0.05$. ADAM17, a disintegrin and metalloprotease 17; DMSO, dimethyl sulfoxide; sVLDLR, soluble ectodomain of VLDLR; VLDLR, very low-density lipoprotein receptor.

ADAM17 responsible for VLDLR shedding

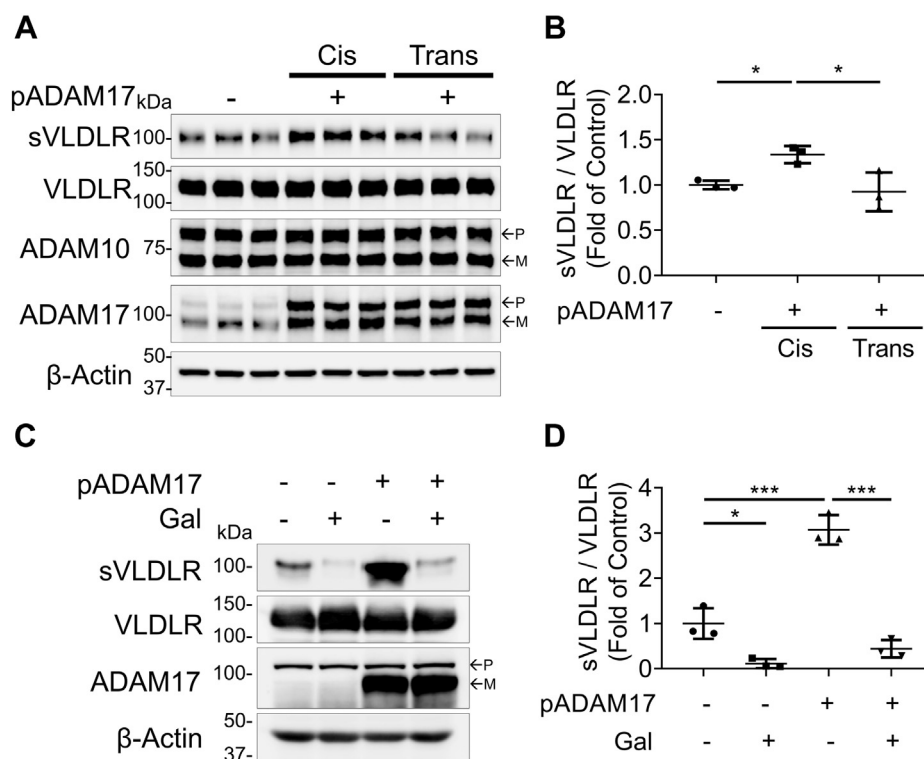


Figure 7. ADAM17 cleaved VLDLR in a *cis* manner, which was blocked by O-glycosylation. Primary human RPE cells were transfected with a plasmid expressing human ADAM17 (pADAM17) or RFP as control for 24 h. Cells were then infected with Ad-VLDLRII (MOI = 25) or RFP as control for another 24 h. After that, the cells were equally split into new 10-cm dishes for comparing *cis* and *trans* manner. *A*, representative images of Western blotting of sVLDLR in culture media, VLDLR, ADAM10, and ADAM17 in ARPE-19 cell lysates. *Cis* indicated that ADAM17 and VLDLR were overexpressed in same cells. *Trans* indicated that ADAM17 and VLDLR were overexpressed in different cells. *B*, densitometry analysis of sVLDLR in culture media normalized by the full-length VLDLR in cell lysates in (A) ($n = 3$). *C*, representative images of Western blotting of sVLDLR in culture media, and VLDLR and ADAM17 in O-glycosylation-deficient cells (ldID). ldID cells were transfected with the ADAM17 expression plasmid (pADAM17) or RFP as control for 24 h. Then, cells were transfected with adenovirus overexpressing VLDLRI, the full-length VLDLR with O-glycosylation domain (MOI = 25) or RFP as control for another 24 h. After that, culture media were replaced with a serum-free media with or without 10 μ M D-(+)-galactose and 100 μ M N-acetyl-D-galactosamine for 24 h. *D*, densitometry analysis of sVLDLR in culture media normalized by VLDLR in cell lysates in (C) ($n = 3$). Gal: D-(+)-galactose and N-acetyl-D-galactosamine. In *A* and *C*, p and m indicated precursor and mature forms of ADAM10 and ADAM17, respectively. Data were presented as mean \pm SD. * $p < 0.05$, *** $p < 0.001$. ADAM10, a disintegrin and metalloprotease 10; ADAM17, a disintegrin and metalloprotease 17; MOI, multiplicity of infection; RFP, red fluorescent protein; RPE, retinal pigment epithelium; VLDLR, very low-density lipoprotein receptor; VLDLRI, VLDLR variant I; VLDLRII, VLDLR variant II.

of the visual cycle (24). As A_2E is accumulated in RPE cells in dry AMD patients, it is commonly used as the oxidant stressor of dry AMD models *in vitro* (25). Hence, we investigated the effect of A_2E on VLDLR shedding in human primary RPE cells. As shown in Figure 8A, A_2E treatment significantly decreased the VLDLR shedding in human RPE cells. Furthermore, we also evaluated the effect of A_2E on ADAM17 expression in human primary RPE cells. We found that A_2E treatment reduced protein levels of ADAM17 in a time-dependent manner (Fig. 8, C and D). These results suggested that A_2E may reduce the level of ADAM17 by blocking protein synthesis or promoting protein degradation of ADAM17.

Therefore, we next measured ADAM17 degradation rate in the A_2E -treated ARPE-19 cells after blocking protein synthesis by cycloheximide (CHX). Upon CHX treatment, the ADAM17 level was decreased in a time-dependent manner (Fig. 8, E and F). A_2E accelerated the decrease of ADAM17 levels relative to the vehicle group (Fig. 8, E and F). On the other hand, MG132 was used to inhibit proteasome activity. With MG132 treatment, protein levels of ADAM17 were increased in a time-dependent manner. Under MG132 treatment, there was no

significant difference of ADAM17 levels between the A_2E -treated group and vehicle group, indicating that MG132 blocked A_2E -induced ADAM17 degradation (Fig. 8, G and H). These results suggested that A_2E reduced ADAM17 levels by accelerating its protein degradation.

Reduced sVLDLR levels and downregulated ADAM17 as well as overactivated Wnt signaling in a mouse model with dry AMD phenotypes

Abca4^{-/-}*Rdh8*^{-/-} mice manifest phenotypes of dry AMD such as A_2E accumulation within RPE, inflammation, oxidative stress, and retinal neuron degeneration (26). Thus, we next investigated if our *in vitro* findings may be replicated in *in vivo* condition. As shown in Figure 9, A and B, there was a decrease of sVLDLR levels in the IPM from 10-month-old *Abca4*^{-/-}*Rdh8*^{-/-} mice. Levels of sVLDLR in the IPM were normalized using amount of total proteins in the IPM stained by Ponceau S. There was no significant difference of the full-length VLDLR in the eyecups between *Abca4*^{-/-}*Rdh8*^{-/-} mice and age-matched WT mice (Fig. S6).

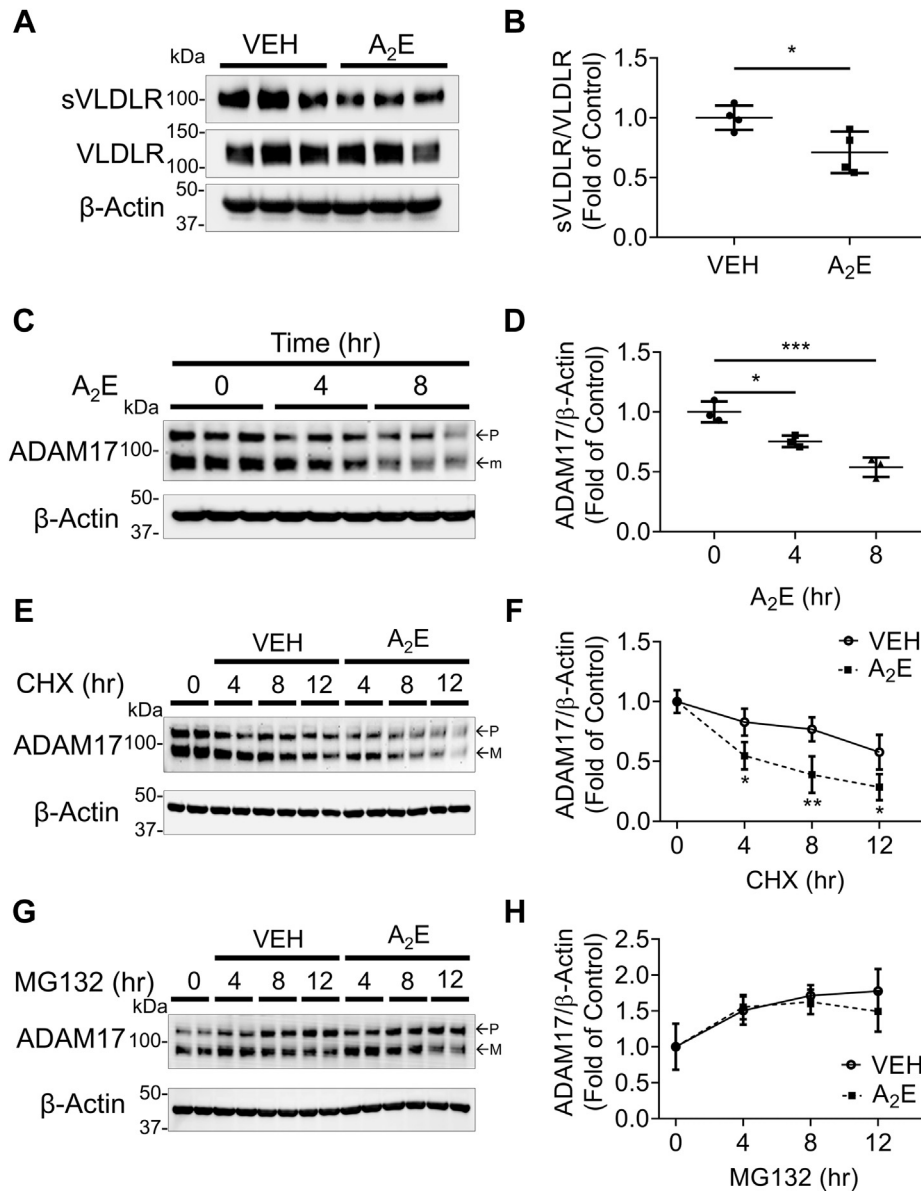


Figure 8. The effect of A₂E on VLDLR shedding and ADAM17 levels. A, representative images of Western blotting of sVLDLR in culture media and VLDLR in primary human RPE cells. Cells were transfected with Ad-VLDLR_{II} (MOI = 25) or Ad-RFP as control for 24 h. The cells were then treated with 50 μM A₂E or vehicle as control for another 24 h. B, protein levels of sVLDLR in culture media in (A) were normalized by VLDLR in cell lysates in (A) (n = 4). C, representative images of Western blotting for ADAM17 in human primary RPE cells treated with A₂E with indicated duration. D, protein levels of ADAM17 in cell lysates in (C) were quantified by densitometry (n = 3). E, representative images of Western blotting for ADAM17 in primary human RPE cells with indicated treatment and duration. Cells were treated with 50 μg/ml cycloheximide (CHX) and/or 50 μM A₂E with indicated duration. F, protein levels of ADAM17 in (E) were quantified by densitometry (n = 3). G, representative images of Western blotting of ADAM17 in primary human RPE cells with indicated treatment and duration. Cells were treated with 10 μM MG132 and/or 50 μM A₂E with indicated duration. H, protein levels of ADAM17 in (G) were quantified by densitometry (n = 3). In C, E, and G, p and m indicated precursor and mature forms of ADAM17, respectively. Data were presented as mean ± SD. *p < 0.05, ***p < 0.001. ADAM17, a disintegrin and metalloprotease 17; MOI, multiplicity of infection; RFP, red fluorescent protein; RPE, retinal pigment epithelium; sVLDLR, soluble ectodomain of VLDLR; VLDLR, very low-density lipoprotein receptor; VLDLR_{II}, VLDLR variant II.

There were significantly lower ADAM17 protein levels in the eyecups of *Abca4*^{-/-}*Rdh8*^{-/-} mice compared with those in age-matched WT mice (Fig. 9, C and D). As measured by ADAM17 activity assay, *Abca4*^{-/-}*Rdh8*^{-/-} mice showed lower ADAM17 activity in the eyecups relative to those in age-matched WT mice (Fig. 9E). These results indicated that deficiency of ADAM17 resulted in the decrease of VLDLR shedding under dry AMD conditions. In addition, there were higher levels of phosphorylated LRP6 and

nonphosphorylated β-catenin in the eyecups of *Abca4*^{-/-}*Rdh8*^{-/-} mice compared with those in age-matched WT mice, suggesting overactivation of Wnt signaling in the eyes of *Abca4*^{-/-}*Rdh8*^{-/-} mice (Fig. 9F). Moreover, immunostaining detected a higher phosphorylated LRP6 intensity and a lower ADAM17 intensity in the RPE region of *Abca4*^{-/-}*Rdh8*^{-/-} mice compared with age-matched WT mice (Fig. 10, A–D). Collectively, these results suggested that downregulation of ADAM17 contributed to decreased

ADAM17 responsible for VLDLR shedding

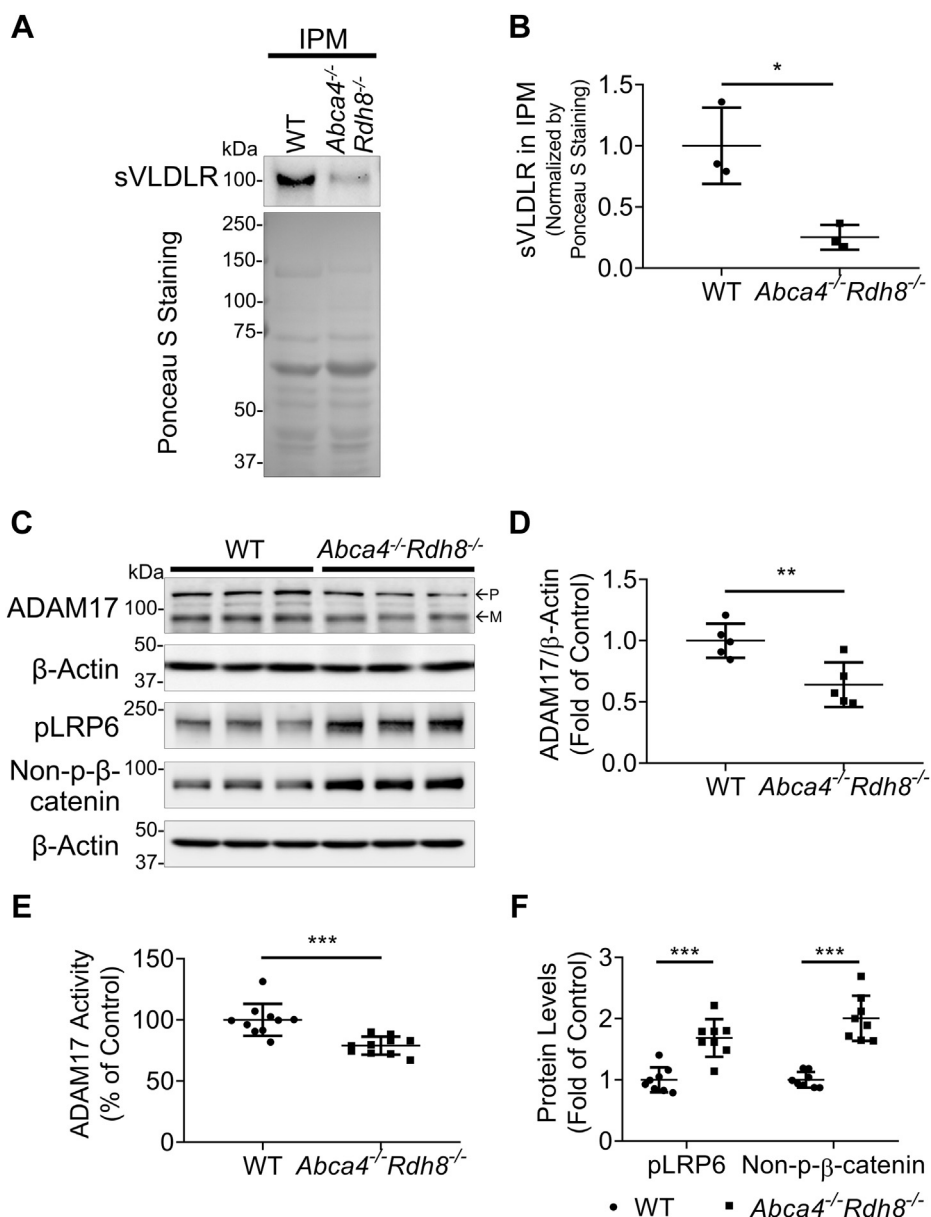


Figure 9. Reduced sVLDLR levels and downregulated ADAM17 were associated with overactivated Wnt signaling in *Abca4*^{-/-}*Rdh8*^{-/-} mice. *A*, representative images of Western blotting of sVLDLR in the IPM and Ponceau S staining of its nitrocellulose membrane. *B*, densitometry quantification of sVLDLR in the IPM normalized by total proteins measured by Ponceau S staining in (A) (*n* = 3). *C*, representative images of Western blotting of ADAM17, phosphorylated LRP6 (pLRP6), and nonphosphorylated β-catenin (non-p-β-catenin) in eyecups of 10-month-old *Abca4*^{-/-}*Rdh8*^{-/-} mice and age-matched WT mice. *D* and *F*, protein levels of ADAM17 (*D*), pLRP6 and non-p-β-catenin (*F*) in (C) were quantified by densitometry (*n* = 5–8). *E*, ADAM17 activity in the eyecups of 10-month-old *Abca4*^{-/-}*Rdh8*^{-/-} mice was measured using ADAM17 activity assay and expressed as percentage of that in age-matched WT mice (*n* = 10). In C, p and m indicated precursor and mature forms of ADAM17, respectively. Data were presented as mean ± SD. **p* < 0.05, ****p* < 0.01, and ****p* < 0.001. ADAM17, a disintegrin and metalloprotease 17; IPM, interphotoreceptor matrix; sVLDLR, soluble ectodomain of VLDLR.

VLDLR shedding into the IPM, leading to aberrant activation of Wnt signaling in subretinal regions of AMD condition.

Discussion

In this study, we identified ADAM17 as the VLDLR shed-dase using pharmacological and genetic approaches. The ADAM17 inhibitor suppressed VLDLR shedding *in vitro* (Fig. 1) and *in vivo* (Fig. 6). Knockdown or KO of ADAM17 expression abolished, whereas overexpression of ADAM17 promoted VLDLR shedding (Figs. 2 and 3). In addition, we

found that ADAM17 promoted sVLDLR-mediated Wnt inhibitory effect and reduced the full-length VLDLR-mediated lipid uptake and ROS generation (Figs. 4 and 5). Moreover, our study unraveled that ADAM17 only cleaved VLDLR in a *cis* manner, and this cleavage was impeded by O-glycosylation in the ectodomain of VLDLR (Fig. 7). This study also showed that an AMD stressor accelerated ADAM17 degradation and reduced VLDLR shedding (Fig. 8). Finally, our results demonstrated that downregulation of ADAM17 was associated with reduced sVLDLR levels and aberrant activation of Wnt signaling of an AMD model (Figs. 9 and 10). These findings

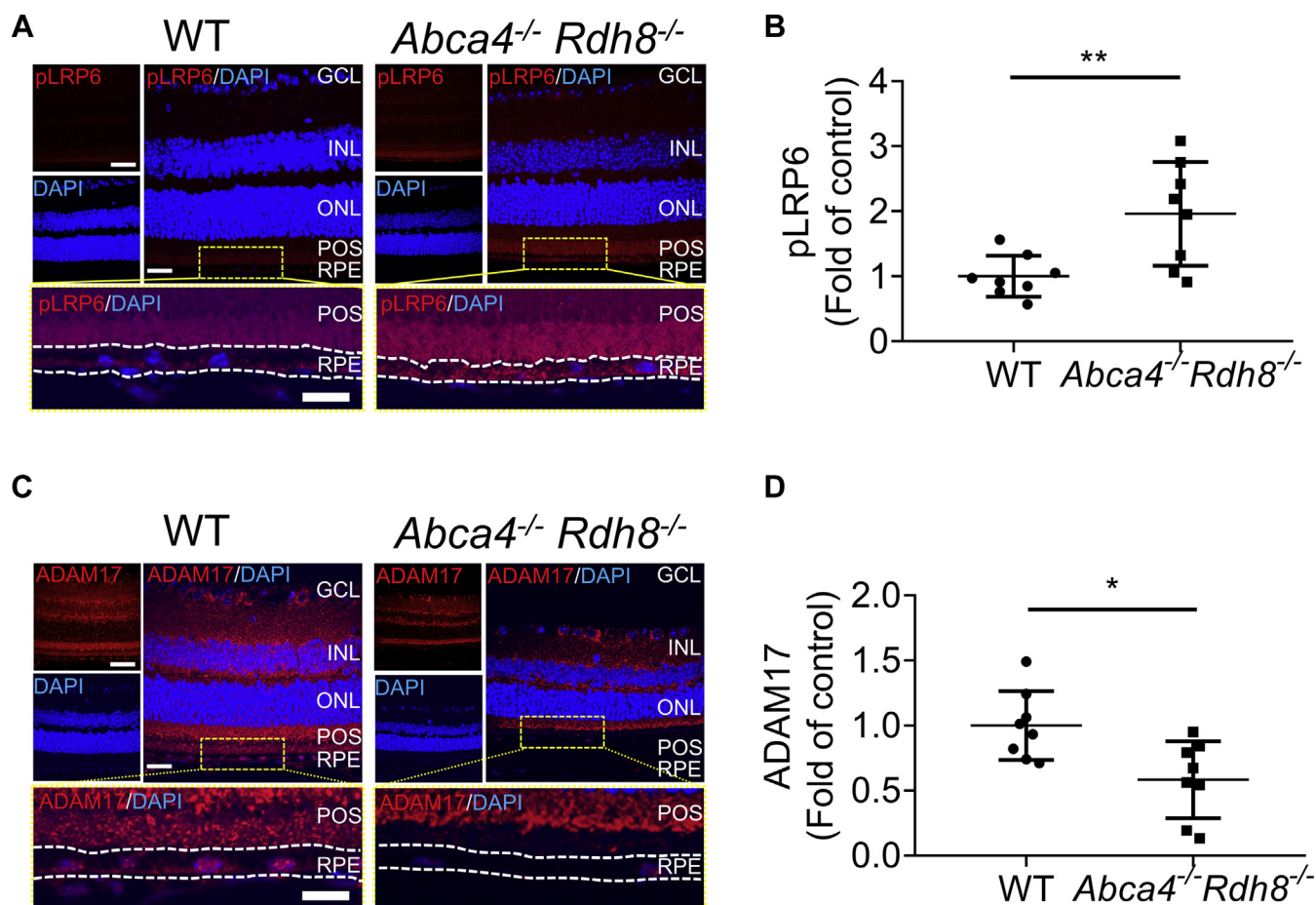


Figure 10. Downregulated ADAM17 and overactivated Wnt signaling were present in the RPE layer of *Abca4*^{-/-}*Rdh8*^{-/-} mice. A, representative images of pLRP6 (red) and DAPI (blue) in retinal sections of 10-month-old *Abca4*^{-/-}*Rdh8*^{-/-} mice and age-matched WT mice. The scale bars represent 80 μ m for upper left image, 40 μ m for upper right image, and 20 μ m for bottom image. B, intensity of pLRP6 in the RPE layer in (A) was quantified using ImageJ (n = 8). C, representative images of ADAM17 (red) and DAPI (blue) in retinal sections of 10-month-old *Abca4*^{-/-}*Rdh8*^{-/-} mice and age-matched WT mice. The scale bars represent 80 μ m for upper left image, 40 μ m for upper right image, and 20 μ m for bottom image. D, intensity of ADAM17 in the RPE layer in (C) was quantified using ImageJ (n = 8). Data were presented as mean \pm SD. **p* < 0.05, ***p* < 0.01. ADAM17, a disintegrin and metalloprotease 17; DAPI, 4',6'-diamino-2-phenylindole; GCL, ganglion cell layer; INL, inner nuclear layer; ONL, outer nuclear layer; POS, photoreceptor outer segment; RPE, retinal pigment epithelium.

unraveled the VLDLR shedding mechanism and may shed light on potential AMD pathogenesis.

Recent proteomic studies have identified a number of substrates for various sheddases, but many of them have not yet been validated under sheddase-deficient conditions or *via in vivo* studies (11). The work by Herzog *et al.* (19) enlightened us with meticulous step-by-step verification of the substrate and its responsible sheddase using proteinase inhibitors with different inhibitory spectra followed by the genetic regulation of sheddase expression. By doing so in human RPE cells, we demonstrated that ADAM17 is the VLDLR sheddase responsible for ectodomain shedding of VLDLR (Fig. 11). VLDLR and ADAM17 are widely expressed in various tissues. We verified that ADAM17 mediated VLDLR shedding in different cell types including photoreceptor cells, kidney cells, and endothelial cells (Fig. S1). In addition, we showed that ADAM17 cleaved both VLDLRI and VLDLR II to shed their ectodomains (Fig. 1 and Fig. S2), suggesting that ADAM17 is responsible for ectodomain shedding in different VLDLR variants. Meanwhile, there was a trace amount of sVLDLR in culture media of

ADAM17 KO cells. Although this trace amount of sVLDLR could arise from cell debris, our study cannot rule out the minor involvement of another unknown sheddase contributing to the VLDLR cleavage.

ADAM17, also referred to as TNF α -converting enzyme, is originally identified as a proteinase responsible for cleaving the transmembrane TNF α precursor (27). Beyond the regulation of TNF α shedding, studies showed that ADAM17 has dozens of substrates (28). As ADAM17 mediates irreversible proteolysis and orchestrates multiple pathophysiological processes, the activity and protein levels of ADAM17 are tightly regulated at multiple levels. There are negative regulators that inhibit the ADAM17 activities, including the prodomain of ADAM17, β -integrin, and TIMP3 (29). Among them, TIMP3 binds with its N terminus to ADAM17 and sterically blocked the interaction between ADAM17 and its substrates (29). As the TIMP3 mutant variants are associated with the onset of AMD (15), it is conceivable that TIMP3 mutants may enhance the binding of TIMP3 with ADAM17, resulting in the abnormal function of ADAM17 and contributing to the AMD

ADAM17 responsible for VLDLR shedding

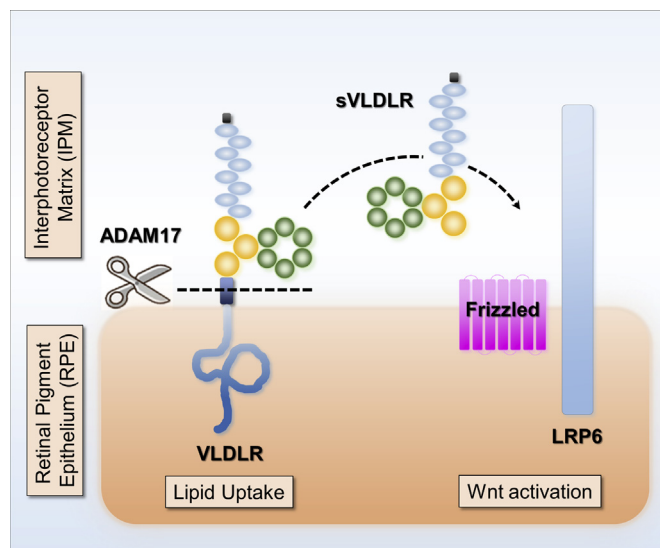


Figure 11. ADAM17-mediated VLDLR shedding modulates Wnt signaling in the eyes. Our previous studies have shown that VLDLR sheds its soluble extracellular domain, sVLDLR, to function as an endogenous inhibitor of canonical Wnt signaling by binding with Wnt receptor, LRP6. However, the sheddase that regulates VLDLR shedding remains unknown. In this study, we found that ADAM17 is the sheddase responsible for VLDLR shedding. ADAM17 liberates sVLDLR and enables its inhibitory effect on Wnt signaling. Meanwhile, ADAM17-mediated VLDLR shedding reduces the lipid uptake through full-length VLDLR. We found that ADAM17 cleaves both variant I and variant II of VLDLR. Future investigation is warranted to study the fate of remaining C terminus of VLDLR. ADAM17, a disintegrin and metalloprotease 17; LRP6, low-density lipoprotein receptor-related protein 6; sVLDLR, soluble ectodomain of VLDLR; VLDLR, very low-density lipoprotein receptor.

pathogenesis. In addition to activity regulators, the ADAM17 regulation could occur on the side of substrates. For instance, O-link glycosylation of VLDLR suppressed ADAM17-mediated shedding activity (Fig. 7). Last, lysosomal-dependent degradation of ADAM17 has an impact on ADAM17 shedding activity (29). As shown in Figure 8, A_2E_1 , a common AMD stressor, promoted ADAM17 degradation, which could be abolished by MG132, the lysosomal proteinase inhibitor. Future investigation is warranted to examine if overexpression of ADAM17 ameliorates AMD phenotypes.

We also characterized the shedding manner of ADAM17 on VLDLR. Previous studies demonstrated that ADAMs may act in both *cis* or *trans* manner to cleave different substrates (30). In this study, our result demonstrated that ADAM17 cleaved VLDLR expressing on the same cell as ADAM17 but not VLDLR on a different cell. In *ADAM17* KO cells, only restored ADAM17 expression in the same cells as that expressed VLDLR resulted in an increase of VLDLR shedding. Given that ADAM17 modulates multiple substrates in various tissues, this result paved the way for tissue-specific regulation of ADAM17-mediated VLDLR shedding in order to avoid potential side effects. In addition, we found that O-glycosylation blocked VLDLR release by ADAM17. Our results showed that ADAM17 overexpression promoted VLDLR shedding in O-glycosylation-deficient cell line. The effect of overexpressed ADAM17 on VLDLR shedding was blocked by the restoration of O-glycosylation. A recent study showed that ADAM17-mediated cleavage was negatively affected by O-glycosylation

in most of the substrates, especially O-glycosylation sites within four amino acid residues from the cleavage sites (31). Further studies regarding O-glycosylation of VLDLR in disorders and identification of cleavage site on VLDLR will provide better understanding of ADAM17-mediated VLDLR shedding.

Among LDLR family members, the structure of VLDLR domains is analogous to that of LDLR, including LDLR type A repeats, epidermal growth factor-like domain, O-glycosylation domain, transmembrane anchor, and cytoplasmic domain (1). Recently, membrane type 1 (MT1) matrix MMP was validated as LDLR sheddase using GM6001, a pan-MMP inhibitor (with the inhibition on MT1-MMP) (32). In the present study, our results showed that GM6001 did not affect the levels of shed sVLDLR in culture media, suggesting that the MMP family, at least MT1-MMP, is not involved in VLDLR shedding. Although LDLR and VLDLR shared highly similar ectodomain, their peptide sequences are different in the juxtamembrane region. This explains why different LDLR family members are cleaved by different sheddases. In addition, although RPE cells have endogenous VLDLR expression (33), the abundance of sVLDLR in the extracellular space is relatively low for shedding study. Therefore, we used adenovirus-mediated VLDLR overexpression system in this study. This system may not fully recapitulate physiological conditions.

The full-length VLDLR mediates lipid uptake by cells. It was conceivable that impaired ADAM17-mediated cleavage of the full-length VLDLR on the plasma membrane contributes to higher lipid uptake into the cells. To study the effect of ADAM17 on lipid uptake, oleic acid was used as it constitutes VLDL, and it is present in extracellular matrix in the eyes (22, 34). Our results showed that loss of ADAM17 promoted VLDLR-mediated lipid accumulation in the cytosol and subsequently increased ROS production in ocular tissues. These results indicated that proper regulation of ADAM17-mediated VLDLR shedding is important for homeostasis of lipid metabolism.

The canonical Wnt signaling profoundly affects multiple pathophysiological processes, including inflammation, oxidative stress, and fibrosis (35, 36). Our previous studies demonstrated that Wnt signaling is overactivated in patients with neovascular AMD and animal models of neovascular AMD (18, 37). However, Wnt signaling in atrophic AMD condition has not been evaluated. The present study provided the first evidence showing that Wnt signaling is overactivated in the eyecups of *Abca4*^{-/-}*Rhd8*^{-/-} mice, suggesting a potential role of Wnt signaling in retinal inflammation and neuronal degeneration in atrophic AMD. Given the vital role of Wnt signaling, it is closely controlled by several endogenous negative regulators, such as Dkk1, kallistatin, and VLDLR (38–40). The present study, through identifying a regulation mechanism for VLDLR shedding, may contribute to the understanding of the complex regulation of Wnt signaling in ocular diseases.

In conclusion, the present study for the first time identified ADAM17 as VLDLR sheddase responsible for VLDLR shedding. ADAM17 cleaved VLDLR ectodomain in a *cis* manner,

which was inhibited by VLDLR O-glycosylation. The ADAM17-mediated VLDLR shedding was impeded under AMD condition, which contributed to overactivation of Wnt signaling in AMD. Further study is warranted to determine if sustained expression of sVLDLR or ADAM17 may attenuate aberrant activation of Wnt signaling and subsequently rescue AMD phenotypes.

Experimental procedures

Reagents

PMA, a PKC activator, TNF α proteinase inhibitor 1, GM6001 (pan-MMP inhibitor), GI254023x (ADAM10 inhibitor), CHX (protein synthesis inhibitor), MG132 (proteasome inhibitor), D-(+)-galactose, and N-acetyl-D-galactosamine were purchased from Sigma-Aldrich. GW280264x (ADAM17 inhibitor) was purchased from Aobious. SensoLyte 520 TNF α -converting enzyme activity assay kit (ADAM17 activity assay kit) was obtained from Anaspec. BODIPY 493/503, phalloidin, and fluorescent dye 2',7'-dichlorodihydrofluorescein diacetate (H2DCFDA) were purchased from Invitrogen.

Cell culture

Human primary RPE cells purchased from Lonza were grown in the retinal pigment epithelial cell growth media (Lonza) supplemented with 2% fetal bovine serum, human fibroblast growth factor B, L-glutamine, and GA-1000 according to the manufacturer's instructions. ARPE-19 cell line, a human RPE cell line, was obtained from the American Type Culture Collection and grown in Dulbecco's modified Eagle's medium/F12 media (Gibco) containing 10% fetal bovine serum, 100 μ g/ml penicillin, and 100 μ g/ml streptomycin. O-glycosylation-deficient Chinese hamster ovary cell line (ldld cell) was cultured following a procedure described previously (10). All cells were routinely cultured in a humidified atmosphere containing 5% CO₂ at 37 °C.

Animals

Abca4^{-/-}*Rdh8*^{-/-} mouse strain was a kind gift from Dr Krzysztof Palczewski (26). To eliminate *Rd8* mutation, *Abca4*^{-/-}*Rdh8*^{-/-} mice were crossbred with WT 129S1/SvImJ (Jackson Laboratory) to generate *Abca4*^{-/-}*Rdh8*^{-/-} mice without *Rd8* mutation in the 129S1/SvImJ background. Age-matched WT 129S1/SvImJ mice were used as control for experiments involved in *Abca4*^{-/-}*Rdh8*^{-/-} mice. C57BL/6J mice were purchased from Jackson Laboratory to verify ADAM17 as the VLDLR sheddase *in vivo*. All procedures using experimental animals strictly followed the protocols approved by the Institute Animal Care and Use Committee at the University of Oklahoma Health Sciences Center. All experiments were performed to comply with the Use of Animals of Association for Research in Vision and Ophthalmology guidelines. Mice were anesthetized with an intraperitoneal injection of a ketamine-xylazine mix (ketamine, 100 mg/kg; xylazine, 5 mg/kg). The pupils were dilated with topical application of cyclopentolate (Akorn). For intravitreal injection, the treatment was delivered using a

33-gauge needle attached to a Nanofil syringe (World Precision Instruments) through an incision on the sclera posterior to the limbus. Ultra-micropump III (World Precision Instruments) was applied to control injection speed at 0.5 μ l/s. After injection, the antibiotic ointment was applied to the sclera to prevent possible infection.

Overexpression of VLDLR

To achieve VLDLR overexpression, cells were transduced with adenovirus expressing VLDLRI (Ad-VLDLRI), VLDLR II (Ad-VLDLR II), or RFP (Ad-RFP) as control (multiplicity of infection = 25). Ad-VLDLRI and Ad-VLDLR II were gifts from Dr Kazuhiro Oka at Baylor College of Medicine, and Ad-RFP was generated as described previously (10). At 24 h post-transduction, culture media were replaced with fresh serum-free media. For screening sheddases by chemical inhibitors, selective sheddase inhibitors were added in the serum-free media at 24 h after virus transduction. At 48 h after Ad-VLDLR transduction, cells and the conditioned media were collected for Western blot analysis.

Overexpression and knockdown of ADAM10 and ADAM17 using plasmids and siRNAs

Expression vectors for human *ADAM10* (Addgene; plasmid #31717) and human *ADAM17* (Addgene; plasmid #31713) were gifts from Dr Rik Derynck (41). SMARTpool human *ADAM10* siRNA and human *ADAM17* siRNA were purchased from Dharmacon. Lipofectamine 2000 (Invitrogen) was used to transfect plasmid vectors (1 μ g/ml) and siRNAs (50 nM) into cells according to the instructions of Invitrogen. At 24 h after transfection, the cells were transduced with Ad-VLDLR as described previously.

Generation of ADAM17 KO cell by CRISPR technology

The guide RNA (gRNA) targeting the human *ADAM17* gene was predicted using online CRISPR/Cas9 design software at <http://crispor.tefor.net>. The targeting sequence for human *ADAM17* was 5'...TTCGTGCTGGCGCCGCGACC...3'. The gRNA of human *ADAM17* was cloned into a CRISPR/Cas9 vector containing the GFP gene in the backbone of the construct (pSpCas9(BB)-2A-GFP; Addgene, #62988) (42). ARPE-19 cells were transfected with a gRNA-inserted CRISPR/Cas9 vector for 48 h. The on-target and off-target effects of designed gRNA were validated using a Surveyor mutation detection kit (Takara Bio). For screening the gene-edited cells, GFP-positive ARPE-19 single cells were sorted into 96-well plates using the FACS Aria Fusion cell sorter (BD Biosciences). After the single cell was expanded and subcultured, *ADAM17* KO efficiency was verified by Western blot analysis. Finally, the genomic DNA sequences of *ADAM17* gene containing gRNA target sites were analyzed by DNA sequencing.

TOPFLASH assay

For the measurement of β -catenin transcriptional activity, a TOPFLASH plasmid containing TCF/lymphoid enhancer-binding factor sites in the promoter upstream of a luciferase

ADAM17 responsible for VLDLR shedding

reporter (Addgene; #12456) and a Renilla luciferase control reporter vector (Promega; #E2231) were cotransfected into ARPE-19 cells as described previously (43). TCF/ β -catenin transcriptional activity was measured using a dual luciferase assay kit in a GloMax 96 microplate luminometer (Promega) and normalized to Renilla luciferase activity. Control conditioned media and Wnt3a conditioned media were harvested from L cells and L cells stably expressing human Wnt3a, respectively (American Type Culture Collection). At 24 h post-transfection, the cells were treated with 20% conditioned media for 16 h and then harvested for TOPFLASH assay following the manufacturer's instruction.

ADAM17 activity assay

The commercial ADAM17 activity assay kit (ANASpec) with fluorogenic substrate QXL520/5-carboxyfluorescein (5-FAM) was used. The fluorescence of 5-FAM is quenched by QXL520 in the intact substrate. In the presence of active ADAM17 from samples, the fluorogenic substrates were cleaved, and fluorescent 5-FAM was released and monitored. Briefly, the cell lysates (10 μ l) were incubated with 50 μ l substrates in 96-well plates at 37 °C for 45 min. The fluorescence signal was then measured at excitation/emission = 485 nm/535 nm using a microplate reader (Wallac Victor 1420; PerkinElmer). The readout was normalized by protein concentrations in cell lysates measured by bicinchoninic acid protein assay (Thermo Fisher Scientific).

Western blot analysis

Western blot analysis was performed as described previously (43). For cell samples, cells were lysed in a cell lysis buffer (50 mM Tris-HCl, pH 6.8, containing 10% glycerol, 2% SDS, and 1% proteinase inhibitor cocktail). The cell lysates were shaken at 4 °C for 1 h and spun at 10,000g for 10 min. The supernatants were collected for sample preparation. For culture media, media were collected and centrifuged at 500g for 5 min to remove the cell debris. For the preparation of tissue samples, the retinas and RPE-choroid complexes were dissected under the microscope and homogenized by the ultrasonic homogenizer. To prepare IPM samples, the IPM was pooled from five mice per group according to a documented protocol (10). Briefly, the retinas and RPE-choroid complexes were separated and gently rinsed with PBS containing 1% proteinase inhibitor cocktail. After that, the PBS was centrifuged at 3000 rpm for 5 min to remove cell debris, and then the supernatants were centrifuged at 70,000 rpm for 1 h to spin down the cell membranes. Finally, the supernatant was collected as the IPM. Protein concentration was determined by bicinchoninic acid assay (Thermo Fisher Scientific), and samples were separated by 8% SDS-PAGE with reducing condition and transferred onto a nitrocellulose membrane. The membrane was blocked with 10% nonfatty milk in Tris-buffered saline with 0.1% Tween-20 for 2 h. Membranes were incubated in primary antibodies at 4 °C overnight and

secondary antibodies for 2 h at room temperature. All antibodies were diluted in Tris-buffered saline with 0.1% Tween-20 containing 5% bovine serum albumin (BSA). Details of primary and secondary antibodies used in this study are shown in Table S1.

Immunohistochemistry

Mouse eyeballs were gently enucleated and fixed in Davidson's fixative for 48 h. Paraffin-embedded eyeball blocks were cut into 5- μ m sections. The deparaffinization and antigen retrieval were performed as described previously (43). The sections were immunostained with primary and secondary antibodies (Table S1). The slides were mounted with the Vectashield mounting buffer containing 4',6'-diamino-2-phenylindole (Vector Laboratories) and then imaged with a laser scanning confocal microscope (FV1000) (Olympus). For the quantification of immunostaining intensity, ImageJ software (The National Institutes of Health) was applied according to a documented protocol (43). Briefly, images were converted to RGB stack, and then the mean gray value was measured in the RPE layer. The values were then normalized to the average value of WT mice. A minimum of six images taken from random fields of six different mice was used for analysis.

Immunocytochemistry and ROS measurement

For the staining of lipid droplets, cells were fixed in PBS containing 3% paraformaldehyde and 0.02% glutaraldehyde for 20 min and then blocked in saponin-containing blocking buffer for 30 min. Tissues were incubated in BODIPY and phalloidin for 2 h. BODIPY was used for staining the lipid droplet, and phalloidin was used to label F-actin as a cytosol indicator. The slides were mounted in SlowFade diamond antifade mountant (Invitrogen) and then imaged with the same confocal microscope mentioned previously. For the quantification of lipid droplet accumulation, ImageJ software was used. Areas of BODIPY staining were quantified by measuring the BODIPY-positive pixels and then were normalized by cell number (4',6'-diamino-2-phenylindole-stained nuclei) in each image using ImageJ. The values were present as fold of control (vehicle group). A minimum of three images taken from random fields of eight replicates were used for analysis. For ROS measurement, WT and ADAM17 KO ARPE19 cells were incubated with H2DCFDA (Invitrogen) for 30 min. Then, the cells were treated with BSA-oleic acid complex (the molar ratio is 1:4) for 16 h, and vehicles were used as control. The H2DCFDA within cells was oxidized to fluorescent dichlorofluorescein (DCF), allowing us to monitor intracellular oxidation status. The DCF fluorescence signal was measured by Wallac Victor 1420 microplate reader. The DCF readout was normalized by the protein concentration in each well. For the staining of DCF, cells were fixed, mounted, and imaged as mentioned previously. For preparing the BSA-oleic acid complex, oleic acid was dissolved in a prewarmed NaOH

solution to form sodium oleate. Then, sodium oleate was mixed with prewarmed PBS containing 10% BSA to form a BSA–oleic acid complex. The reagent was adjusted to pH 7.4 and filtered for sterilization. The vehicle containing BSA was used as a control.

Statistical analysis

Experiments were performed at least three times separately for *in vitro* experiments, and at least six mice per group were used for the animal experiments. Results were presented as the mean \pm SD. Statistical analyses were performed using the two-tailed Student's *t* test to compare two groups, or ANOVA followed by the Student–Newman–Keuls test when more than two groups was compared. A *p* value of <0.05 was considered statistically significant.

Data availability

All data are contained within this article. Reagents and plasmids described in this article are available upon request.

Supporting information—This article contains [supporting information](#) (7).

Acknowledgments—This study was supported by the National Institutes of Health grants (EY019309, EY012231, EY028949, EY032930, and EY032931). The content is solely the responsibility of the authors and does not necessarily represent the official views of the National Institutes of Health. The authors like to thank the technical support from the Diabetic Animal Core and Histology and Image Core of diabetic COBRE (GM122744) and the Vision Core supported by NEI P30 (EY021725). In addition, Dr Qian Chen at Xiamen University provided kind assistance and critical discussion in this project.

Author contributions—X. M., Y. T., and J.-X. M. conceptualization; X. M., Y. T., W. W., W. L., J. C., Y. L., and Y. D. methodology; X. M. and W. L. validation; X. M. formal analysis; X. M. and D. C. investigation; X. M., W. W., W. L., Y. L., and Y. D. resources; X. M., J. C., and D. C. data curation; X. M. writing—original draft; Y. T., S. B., and J.-X. M. writing—review and editing; X. M. visualization; Y. T., J. C., S. B., and J.-X. M. supervision; X. M. project administration.

Conflict of interest—The authors declare that they have no conflicts of interest with the contents of this article.

Abbreviations—The abbreviations used are: 5-FAM, 5-carboxyfluorescein; ADAM17, a disintegrin and metalloprotease 17; AMD, age-related macular degeneration; BSA, bovine serum albumin; CHX, cycloheximide; DCF, dichlorofluorescein; gRNA, guide RNA; H2DCFDA, 2',7'-dichlorodihydrofluorescein diacetate; IPM, interphotoreceptor matrix; LDLR, low-density lipoprotein receptor; LRP6, low-density lipoprotein receptor–related protein 6; MMP, matrix metalloproteinase; MT1, membrane type 1; PKC, protein kinase C; PMA, phorbol 12-myristate 13-acetate; RFP, red fluorescent protein; ROS, reactive oxygen species; RPE, retinal pigment epithelium; sVLDLR, soluble ectodomain of VLDLR; TCF, T-cell factor; TIMP3, tissue inhibitor of metalloproteinase 3; TNF α ,

tumor necrosis factor alpha; VLDLR, very low-density lipoprotein receptor; VLDLRI, VLDLR variant I; VLDLRII, VLDLR variant II.

References

- Go, G. W., and Mani, A. (2012) Low-density lipoprotein receptor (LDLR) family orchestrates cholesterol homeostasis. *Yale J. Biol. Med.* **85**, 19–28
- Argaves, W. S. (2001) Members of the low density lipoprotein receptor family control diverse physiological processes. *Front. Biosci.* **6**, D406–D416
- Nguyen, A., Tao, H., Metrione, M., and Hajri, T. (2014) Very low density lipoprotein receptor (VLDLR) expression is a determinant factor in adipose tissue inflammation and adipocyte-macrophage interaction. *J. Biol. Chem.* **289**, 1688–1703
- Dlugosz, P., and Nimpf, J. (2018) The Reelin receptors apolipoprotein E receptor 2 (ApoER2) and VLDL receptor. *Int. J. Mol. Sci.* **19**, 3090
- Leeb, C., Eresheim, C., and Nimpf, J. (2014) Clusterin is a ligand for apolipoprotein E receptor 2 (ApoER2) and very low density lipoprotein receptor (VLDLR) and signals via the Reelin-signaling pathway. *J. Biol. Chem.* **289**, 4161–4172
- Chen, Y., Hu, Y., Lu, K., Flannery, J. G., and Ma, J. X. (2007) Very low density lipoprotein receptor, a negative regulator of the Wnt signaling pathway and choroidal neovascularization. *J. Biol. Chem.* **282**, 34420–34428
- Lee, K., Shin, Y., Cheng, R., Park, K., Hu, Y., McBride, J., He, X., Takahashi, Y., and Ma, J. X. (2014) Receptor heterodimerization as a novel mechanism for the regulation of Wnt/beta-catenin signaling. *J. Cell Sci.* **127**, 4857–4869
- Chen, Y., Hu, Y., Moiseyev, G., Zhou, K. K., Chen, D., and Ma, J. X. (2009) Photoreceptor degeneration and retinal inflammation induced by very low-density lipoprotein receptor deficiency. *Microvasc. Res.* **78**, 119–127
- Sakai, K., Tiebel, O., Ljungberg, M. C., Sullivan, M., Lee, H. J., Terashima, T., Li, R., Kobayashi, K., Lu, H. C., Chan, L., and Oka, K. (2009) A neuronal VLDLR variant lacking the third complement-type repeat exhibits high capacity binding of apoE containing lipoproteins. *Brain Res.* **1276**, 11–21
- Chen, Q., Takahashi, Y., Oka, K., and Ma, J. X. (2016) Functional differences of very-low-density lipoprotein receptor splice variants in regulating Wnt signaling. *Mol. Cell. Biol.* **36**, 2645–2654
- Lichtenthaler, S. F., Lemberg, M. K., and Fluhner, R. (2018) Proteolytic ectodomain shedding of membrane proteins in mammals—hardware, concepts, and recent developments. *EMBO J.* **37**, e99456
- Murphy, G. (2008) The ADAMs: Signalling scissors in the tumour microenvironment. *Nat. Rev. Cancer* **8**, 929–941
- Mitchell, P., Liew, G., Gopinath, B., and Wong, T. Y. (2018) Age-related macular degeneration. *Lancet* **392**, 1147–1159
- Cheung, C. M., and Wong, T. Y. (2013) Treatment of age-related macular degeneration. *Lancet* **382**, 1230–1232
- Fritsche, L. G., Igl, W., Bailey, J. N., Grassmann, F., Sengupta, S., Bragg-Gresham, J. L., Burdon, K. P., Hebbaring, S. J., Wen, C., Gorski, M., Kim, I. K., Cho, D., Zack, D., Souied, E., Scholl, H. P., *et al.* (2016) A large genome-wide association study of age-related macular degeneration highlights contributions of rare and common variants. *Nat. Genet.* **48**, 134–143
- Campbell, M. A., Sarohia, G. S., Campbell, M., Cui, J. Z., and Matsubara, J. A. (2019) The presence of ADAMs in the eye: Exploring a promising therapeutic target for age-related macular degeneration. *Invest. Ophthalmol. Vis. Sci.* **60**, 1239
- Muliyil, S., Levett, C., Düsterhöft, S., Dulloo, I., Cowley, S. A., and Freeman, M. (2020) ADAM17-triggered TNF signalling protects the ageing Drosophila retina from lipid droplet-mediated degeneration. *EMBO J.* **39**, e104415
- Tuo, J., Wang, Y., Cheng, R., Li, Y., Chen, M., Qiu, F., Qian, H., Shen, D., Penalva, R., Xu, H., Ma, J. X., and Chan, C. C. (2015) Wnt signaling in age-related macular degeneration: Human macular tissue and mouse model. *J. Transl. Med.* **13**, 330

ADAM17 responsible for VLDLR shedding

19. Herzog, C., Haun, R. S., Ludwig, A., Shah, S. V., and Kaushal, G. P. (2014) ADAM10 is the major sheddase responsible for the release of membrane-associated meprin A. *J. Biol. Chem.* **289**, 13308–13322
20. Lorenzen, I., Lokau, J., Korpys, Y., Oldefest, M., Flynn, C. M., Künzel, U., Garbers, C., Freeman, M., Grötzinger, J., and Düsterhöft, S. (2016) Control of ADAM17 activity by regulation of its cellular localisation. *Sci. Rep.* **6**, 35067
21. Hundhausen, C., Misztela, D., Berkhout, T. A., Broadway, N., Saftig, P., Reiss, K., Hartmann, D., Fahrenholz, F., Postina, R., Matthews, V., Kallen, K. J., Rose-John, S., and Ludwig, A. (2003) The disintegrin-like metalloproteinase ADAM10 is involved in constitutive cleavage of CX3CL1 (fractalkine) and regulates CX3CL1-mediated cell-cell adhesion. *Blood* **102**, 1186–1195
22. Ishikawa, M., Sawada, Y., and Yoshitomi, T. (2015) Structure and function of the interphotoreceptor matrix surrounding retinal photoreceptor cells. *Exp. Eye Res.* **133**, 3–18
23. Fuhrmann, S., Zou, C., and Levine, E. M. (2014) Retinal pigment epithelium development, plasticity, and tissue homeostasis. *Exp. Eye Res.* **123**, 141–150
24. Perusek, L., Sahu, B., Parmar, T., Maeno, H., Arai, E., Le, Y. Z., Subauste, C. S., Chen, Y., Palczewski, K., and Maeda, A. (2015) Di-retinoid-pyridinium-ethanolamine (A2E) accumulation and the maintenance of the visual cycle are independent of Atg7-mediated autophagy in the retinal pigmented epithelium. *J. Biol. Chem.* **290**, 29035–29044
25. Kiser, P. D., Golczak, M., and Palczewski, K. (2014) Chemistry of the retinoid (visual) cycle. *Chem. Rev.* **114**, 194–232
26. Maeda, A., Maeda, T., Golczak, M., and Palczewski, K. (2008) Retinopathy in mice induced by disrupted all-trans-retinal clearance. *J. Biol. Chem.* **283**, 26684–26693
27. Moss, M. L., Jin, S. L., Milla, M. E., Bickett, D. M., Burkhart, W., Carter, H. L., Chen, W. J., Clay, W. C., Didsbury, J. R., Hassler, D., Hoffman, C. R., Kost, T. A., Lambert, M. H., Leesnitzer, M. A., McCauley, P., et al. (1997) Cloning of a disintegrin metalloproteinase that processes precursor tumour-necrosis factor- α . *Nature* **385**, 733–736
28. Gooz, M. (2010) ADAM-17: The enzyme that does it all. *Crit. Rev. Biochem. Mol. Biol.* **45**, 146–169
29. Grötzinger, J., Lorenzen, I., and Düsterhöft, S. (2017) Molecular insights into the multilayered regulation of ADAM17: The role of the extracellular region. *Biochim. Biophys. Acta Mol. Cell Res.* **1864**, 2088–2095
30. Buchanan, P. C., Boylan, K. L. M., Walcheck, B., Heinze, R., Geller, M. A., Argenta, P. A., and Skubitz, A. P. N. (2017) Ectodomain shedding of the cell adhesion molecule nectin-4 in ovarian cancer is mediated by ADAM10 and ADAM17. *J. Biol. Chem.* **292**, 6339–6351
31. Goth, C. K., Halim, A., Khetarpal, S. A., Rader, D. J., Clausen, H., and Schjoldager, K. T. (2015) A systematic study of modulation of ADAM-mediated ectodomain shedding by site-specific O-glycosylation. *Proc. Natl. Acad. Sci. U. S. A.* **112**, 14623–14628
32. Alabi, A., Xia, X. D., Gu, H. M., Wang, F., Deng, S. J., Yang, N., Adijiang, A., Douglas, D. N., Kneteman, N. M., Xue, Y., Chen, L., Qin, S., Wang, G., and Zhang, D. W. (2021) Membrane type 1 matrix metalloproteinase promotes LDL receptor shedding and accelerates the development of atherosclerosis. *Nat. Commun.* **12**, 1889
33. Hu, W., Jiang, A., Liang, J., Meng, H., Chang, B., Gao, H., and Qiao, X. (2008) Expression of VLDLR in the retina and evolution of subretinal neovascularization in the knockout mouse model's retinal angiomatous proliferation. *Invest. Ophthalmol. Vis. Sci.* **49**, 407–415
34. Heath, R. B., Karpe, F., Milne, R. W., Burdge, G. C., Wootton, S. A., and Frayn, K. N. (2007) Dietary fatty acids make a rapid and substantial contribution to VLDL-triacylglycerol in the fed state. *Am. J. Physiol. Endocrinol. Metab.* **292**, E732–E739
35. Ma, B., and Hottiger, M. O. (2016) Crosstalk between Wnt/ β -catenin and NF- κ B signaling pathway during inflammation. *Front. Immunol.* **7**, 378
36. Burgy, O., and Konigshoff, M. (2018) The WNT signaling pathways in wound healing and fibrosis. *Matrix Biol.* **68–69**, 67–80
37. Hu, Y., Chen, Y., Lin, M., Lee, K., Mott, R. A., and Ma, J. X. (2013) Pathogenic role of the Wnt signaling pathway activation in laser-induced choroidal neovascularization. *Invest. Ophthalmol. Vis. Sci.* **54**, 141–154
38. Wang, Z., Cheng, R., Lee, K., Tyagi, P., Ding, L., Kompella, U. B., Chen, J., Xu, X., and Ma, J. X. (2015) Nanoparticle-mediated expression of a Wnt pathway inhibitor ameliorates ocular neovascularization. *Arterioscler. Thromb. Vasc. Biol.* **35**, 855–864
39. Semenov, M. V., Zhang, X., and He, X. (2008) DKK1 antagonizes Wnt signaling without promotion of LRP6 internalization and degradation. *J. Biol. Chem.* **283**, 21427–21432
40. Liu, X., Zhang, B., McBride, J. D., Zhou, K., Lee, K., Zhou, Y., Liu, Z., and Ma, J. X. (2013) Antiangiogenic and antineuroinflammatory effects of kallistatin through interactions with the canonical Wnt pathway. *Diabetes* **62**, 4228–4238
41. Liu, C., Xu, P., Lamouille, S., Xu, J., and Derynck, R. (2009) TACE-mediated ectodomain shedding of the type I TGF- β receptor down-regulates TGF- β signaling. *Mol. Cell* **35**, 26–36
42. Ran, F. A., Hsu, P. D., Wright, J., Agarwala, V., Scott, D. A., and Zhang, F. (2013) Genome engineering using the CRISPR-Cas9 system. *Nat. Protoc.* **8**, 2281–2308
43. Qiu, F., Ma, X., Shin, Y. H., Chen, J., Chen, Q., Zhou, K., Wu, W., Liang, W., Wu, Y., Song, Q., and Ma, J. X. (2020) Pathogenic role of human C-reactive protein in diabetic retinopathy. *Clin. Sci. (Lond.)* **134**, 1613–1629